

Comparative evaluation of the fractional flow reserve derived from coronary computed tomography angiography (CT-FFR) and fat attenuation index (FAI) in predicting revascularization

Fengfeng Yang

Tianjin Medical University Second Hospital: The Second Hospital of Tianjin Medical University

Chentao Zhu

Fourth Affiliated Hospital of Harbin Medical University

Ke Shi

Fourth Affiliated Hospital of Harbin Medical University

Yang Zhao

Tianjin Medical University Second Hospital: The Second Hospital of Tianjin Medical University

Tong Zhang (✉ zhangt0415@163.com)

Fourth Affiliated Hospital of Harbin Medical University

Research article

Keywords: coronary CT angiography, CT-FFR, FAI, revascularization, PCAT

Posted Date: November 30th, 2022

DOI: <https://doi.org/10.21203/rs.3.rs-2116172/v1>

License:   This work is licensed under a Creative Commons Attribution 4.0 International License.

[Read Full License](#)

Abstract

Purpose

This study aimed to evaluate the clinical value of the fractional flow reserve derived from coronary computed tomography angiography (CT-FFR) and fat attenuation index (FAI) in predicting coronary revascularization.

Methods

Patients with known or suspected CAD who underwent coronary computed tomography angiography (CCTA) and subsequent invasive coronary angiography were screened. All CCTA data were calculated by a cloud workstation in standard Digital Imaging and Communications in Medicine format. Lesion-specific CT-FFR, distal-tip CT-FFR, and FAI were analyzed by core laboratories blinded to patient management.

Results

A total of 94 patients who received CCTA followed by invasive coronary angiography were identified and analyzed; 282 vessels were included for analysis. Overall, 54 (57.4%) patients with 72(25.5%) vessels demonstrated revascularization. In the multivariate model, FAI (odds ratio [OR]: 1.19; $p < 0.001$), lesion-specific CT-FFR (OR: 3.80; $p = 0.009$), and distal-tip CT-FFR (OR: 4.20; $p = 0.008$) values were identified as independent negative predictors. All receiver operating characteristic curves were above the reference line. The areas under the receiver operating characteristic curve for lesion-specific CT-FFR, distal-tip CT-FFR, and FAI were 0.798, 0.767, and 0.802, respectively. When the optimal threshold value of FAI was -86 HU, the sensitivity, specificity, positive predictive value, negative predictive value, and overall accuracy for predicting revascularization were 88.9%, 59.0%, 42.7%, 93.2%, and 0.66, respectively. The corresponding values for the lesion-specific CT-FFR were 73.6%, 81.0%, 56.3%, 88.2%, and 0.78, respectively.

Conclusions

In patients with documented CAD on CCTA, adjunctive noninvasive functional testing based on the CT-FFR and FAI yielded similar overall accuracy for prediction of coronary revascularization. However, a significant difference was observed in diagnostic sensitivity of the FAI; the lesion-specific CT-FFR demonstrated the highest specificity. In conclusion, CT-FFR and FAI derived from quantitative CCTA improved the prediction of future revascularization. These parameters can potentially identify patients likely to require revascularization on referral for cardiac catheterization.

Introduction

Invasive coronary angiography (ICA) is the gold standard for evaluation of the coronary artery lumen. However, the low diagnostic yield of ICA poses a problem in cardiology. In 2010, a major study revealed that only 37% of patients receiving ICA had $\geq 50\%$ stenosis [21]. According to previous research, the lack of non-invasive testing for patients at low-to-moderate risk for coronary artery disease (CAD) may contribute to the low diagnostic yield of ICA [21]. Over the past three decades, coronary computed tomography angiography (CCTA) has emerged as a robust and reliable non-invasive imaging modality for the assessment of CAD [13]. Although it is increasingly playing the role of a gatekeeper during referral for ICA [24], further optimization is needed. The PROMISE trial showed that CCTA results in a higher rate of ICA than functional testing in symptomatic patients with suspected CAD. Coronary intervention was performed in only half of the cases, despite the presence of $\geq 50\%$ stenosis on ICA in the majority of cases [7]. Additionally, CCTA could not evaluate the hemodynamic significance of the lesions. The fractional flow reserve derived from coronary computed tomography angiography (CT-FFR) is a new technique that combines computer imaging reconstruction and functional analysis by fluid dynamics simulation [8; 26]. Many studies have reported that CT-FFR offers higher diagnostic accuracy than other non-invasive examination modalities for heart disease under the reference of the gold standard invasive FFR[25; 27].

CAD is pathologically characterized by the accumulation of atherosclerotic plaques in the walls of the coronary arteries. As vascular inflammation is a major driver of atherogenesis and thrombosis, it is believed to play a key role in the pathogenesis and progression of CAD [29]. The appearance of epicardial adipose tissue on CT has recently been identified as a noninvasive marker of vascular inflammation, because proinflammatory signals released from epicardial adipose tissue contribute to atherogenesis. Recent studies have shown that vascular inflammation may inhibit lipid accumulation in pericoronary adipose tissue (PCAT); this could be detected as an increase in CT attenuation of PCAT around the proximal coronary artery using CCTA [2]. A non-invasive biomarker proposed to be useful in the detection of coronary inflammation is the fat attenuation index (FAI), which captures CT attenuation changes in PCAT and further reveals changes in PCAT composition induced by vascular inflammation [2]. Recent studies suggest a relationship between elevated FAI and hemodynamically relevant coronary stenosis [12; 30].

To the best of our knowledge, research on the application of CT-FFR and FAI values in predicting coronary revascularization are lacking. Patients who do not undergo revascularization after being referred for cardiac catheterization based on CCTA represent a high-cost population with low yield from the invasive procedure. It would therefore be beneficial to effectively identify these patients [15]. In order to improve the role of CCTA as a doorman, it is essential to find a safe and effective method for reducing the proportion of patients who do not receive intervention. The purpose of this study was to evaluate the clinical value of quantitative parameters, namely, CT-FFR and FAI derived from CCTA, in predicting coronary revascularization.

Methods

2.1 Patients

In the present study, 123 patients with known or suspected CAD who underwent CCTA and subsequent ICA between July 2021 and June 2022 were screened. The exclusion criteria were as follows: patients with a history of coronary stenting or coronary artery bypass grafting, renal insufficiency with a baseline creatinine level of > 2.0 mg/dL, congestive heart failure, and cardiogenic shock; patients with suboptimal image quality were also excluded. A total of 94 patients with a diagnosis of known or suspected CAD as per the registry were included in the final analysis. The study was conducted in accordance with the Declaration of Helsinki (as revised in 2013), and was approved by the Medical Ethics Committee. The need for informed consent was waived for this retrospective study. Figure 1 shows a detailed time line of the study protocol.

2.2 Coronary Cta

The Toshiba 320-row CT (Aquilion ONE, Toshiba, Tokyo, Japan) scanner was used for data acquisition. In patients with heart rates exceeding 80 beats/min, 25–50 mg metoprolol was administered orally; scanning was performed after the heart rate was reduced to below 70 beats/min. An indwelling 18-G trocar was placed in the antecubital vein, and non-ionic iodine contrast medium (350 mg/L) was injected using a two chamber high pressure injector (Mallinckrodt Pharmaceuticals, Staines-upon-Thames, UK); patients with a body mass index of < 25 kg/m² were administered 60 mL of the contrast medium at a rate of 4.0-4.5 mL/s, while those with a body mass index of 25–35 kg/m² were administered a volume of 70 mL at a rate of 4.5-5.0 mL/s. The 320 detector-row CT images were acquired with a gantry rotation time of 350 ms and a tube voltage of 120 kV; the radiation dose was 1.0 ± 0.5 mSv. The best phase was reconstructed retrospectively, with reformat thicknesses and intervals of 0.5 mm, each. The collected data were transferred to the Vitrea FX workstation (Canon Medical, Japan) for post-processing; this included multi-planar reformatting, curved multi-planar reformatting, and volume reformatting, among others.

Image quality was categorized into four grades: poor, medium, good, and excellent. Only images with good to excellent quality were included for further analysis. All CT images were analyzed separately by two experienced senior radiologists. In cases where there was a difference in opinion, a final conclusion was drawn after detailed discussion. The coronary tree was assessed based on the 18-segment coronary artery segmentation system published by the American Society for Cardiovascular Computed Tomography in 2014; the severity of stenosis at each segment was assessed visually, and patients were classified according to the Coronary Artery Disease Reporting and Data System [16]. Stenosis degree was categorized into six grades, as follows: 0, no stenosis; 1, slight stenosis (stenosis < 25%); 2, mild stenosis (stenosis degree 25% ~ 49%); 3, moderate stenosis (stenosis degree 50%-69%); 4. Severe stenosis (70% ~ 99% stenosis); and 5, occlusion (stenosis degree 100%) [5]. Obvious obstructive CAD was defined by stenosis of ≥ 50% of the vessel diameter.

2.3 Ct-ffr Analysis

Artificial intelligence deep learning-based software (Shukun Technology Co., Ltd.) was utilized for the calculation of CT-FFR in this study[11]. This deep learning algorithm calculates the CT-FFR from the reduced-order method combined with machine learning modification[9; 18]. The centerline is completely automatic and no manual related to changing something is needed though the whole pipeline. No user action that helps a bad situation also means that the results are working regularly without black-and-white bias.

All CCTA data were transmitted to the cloud workstation in standard Digital Imaging and Communications in Medicine format. The software calculated and obtained the blood flow reserve fraction based on the training and learning of fluid dynamics simulation data from a large number of coronary cases; the output time was < 10 min per case. The software provided a specific three-dimensional model of the coronary arteries, allowing the investigator to obtain CT-FFR values along any given point along the length of the coronary vessels.

The lesion-specific CT-FFR (at 2 cm distal to the stenosis) after coronary artery stenosis was recorded for each vessel; if the CT-FFR value was ≤ 0.8 , the patient was classified as having obstructive CAD (Fig. 2). The distal-tip CT-FFR (the CT-FFR value at the distal end of each vessel) was also recorded using the same ischemia threshold corresponding to the location of coronary artery stenosis and corresponding 3D coronary artery model (Fig. 2).

2.4 Fai Analysis

FAI analysis closely followed the methodology previously defined by Oikanomou et al.; it was performed using CoronaryDoc (Shukun Technology). The measurement of PCAT attenuation around the proximal right coronary artery (RCA) is a standardized method; this parameter has been used in prior studies as a representative biomarker of coronary inflammation [19]. The proximal 40-mm segment of the left anterior descending coronary artery (LAD), left circumflex coronary artery (LCx), and RCA were traced, as previously described [2; 10]. The lumen and inner and outer vessel wall borders were tracked within the pre-identified segment of interest in an automated manner with additional manual optimization. PCAT was defined as the adipose tissue located around the outer vessel wall, within a radial distance equal to the coronary vessel diameter. Voxel histograms of CT attenuation were plotted and the mean CT attenuation of all voxels ranging between - 190 to - 30 HU (threshold used for defining adipose tissue [19]) within the PCAT volume was calculated. The FAI was defined as the mean CT attenuation of PCAT in the traced 40-mm segment on crude analysis. Representative images of FAI analysis are shown in Fig. 2. PCAT analysis was performed by investigators who were blinded to clinical data.

2.5 Ica And Revascularization

The primary endpoint in our study was revascularization during or directly after referral for ICA; this included percutaneous coronary revascularization and coronary artery bypass grafting. Secondary

analysis involved the prediction of lesion-specific ischemia ($\text{FFR} \leq 0.80$) and revascularization within the sub-cohort of patients who received invasive FFR during ICA. The procedure was performed by two cardiologists with at least 10 years' experience.

Statistical Analysis

SPSS 20.0 (SPSS, Inc., Chicago, IL, USA) and MedCalc 15.6 (MedCalc Software, Mariakerke, Belgium) software packages were used for all statistical analyses. Normally and non-normally distributed continuous variables have been presented as means with standard deviation and medians with interquartile ranges, respectively. The Student's t- and Mann-Whitney U tests were used for normally and non-normally distributed data, respectively; the chi-square test was used for categorical variables. Univariable and multivariable analyses were performed on both per-patient and per-vessel basis. Receiver operating characteristic (ROC) curves were constructed using the CT-FFR and FAI to establish the optimal threshold values for predicting revascularization using CCTA. The diagnostic capability was determined by calculating the area under the ROC curve (AUC); the DeLong method was used for comparison of AUCs. The optimal threshold value was determined according to the highest Youden's J statistic. In cases where the optimal threshold value was adopted, the sensitivity, specificity, positive predictive value (PPV), negative predictive value (NPV), and accuracy with corresponding 95% confidence intervals (CIs) were calculated for these quantitative parameters. P values < 0.05 were considered statistically significant.

Results

Per-patient and per-vessel univariable analysis

A total of 94 patients who underwent CCTA followed by ICA were identified and analyzed; 282 vessels were included in the analysis (Table 1 and Table 2). The mean age was 61.8 ± 7.9 years and 66.0% of patients were male; the mean body mass index was $25.2 \pm 1.4 \text{ kg/m}^2$.

Overall, 54 (57.4%) patients underwent revascularization; 38 (40.4%), 13 (13.8%), and 3 (3.2%) patients underwent revascularization of 1, 2, and 3 vessels, respectively. None of the patients with < 50% stenosis underwent revascularization; 5 patients underwent coronary artery bypass grafting and the others received percutaneous coronary intervention therapy (Table 1).

A total of 72 (25.5%) vessels were revascularized; the vessels included the LAD, LCx, and RCA in 34 (12.1%), 15 (5.3%), and 23 (8.2%) cases, respectively (Table 2). Details pertaining to the number of revascularized vessels with the measured lesion-specific CT-FFR, distal-tip CT-FFR, and FAI are shown in Table 2.

Ct-ffr Analysis

The mean lesion-specific CT-FFR values in revascularized and non-revascularized vessels were 0.7564 (95% CI: 0.7265–0.7862) and 0.8975 (95% CI: 0.8841–0.9110), respectively; $P < 0.0001$ (Table 3 and Fig. 3). The mean distal-tip CT-FFR values in revascularized and non-revascularized vessels were 0.7099 (95% CI: 0.6769–0.7429) and 0.8506 (95% CI: 0.8340–0.8672), respectively; $P < 0.0001$ (Table 4 and Fig. 4). We had also compared the lesion-specific CT-FFR and distal-tip CT-FFR values of 282 vessels. The mean lesion-specific CT-FFR value was 0.8615 (95% CI: 0.8471–0.8759) and the mean distal-tip CT-FFR value was 0.8147 (95% CI: 0.7982–0.8312); $P < 0.0001$ (Table 5). Overall, the distal-tip CT-FFR value was less than the lesion-specific CT-FFR value (Fig. 5).

Fai Analysis

The mean FAI values in the revascularization and non-revascularization groups were -78.0833 (95% CI: -79.7611 - -76.4055) and -87.1714 (95% CI: -88.2800 - -86.0629), respectively; $P < 0.0001$ (Table 6). In the sub vascular groups, the mean FAI values of the LAD ($P < 0.011$), LCx ($P < 0.0001$), and RCA ($P < 0.0001$) differed significantly between the revascularization and non-revascularization groups (Fig. 6). The mean FAI values of all vessels and sub vascular groups were higher in the revascularization group than in the non-revascularization group (Fig. 6).

Multivariate Analysis

On multivariate analysis, the identified independent negative predictors were the FAI (odds ratio [OR]: 1.19; 95% CI: 1.12 to 1.25; $p < 0.001$), lesion-specific CT-FFR value (OR: 3.80; 95% CI: 1.40 to 10.34; $p = 0.009$), and distal-tip CT-FFR value (OR: 4.20; 95% CI: 1.46 to 12.07; $p = 0.008$) (Table 7).

Prediction Of Revascularization

ROC curves of the lesion-specific CT-FFR, distal-tip CT-FFR, and FAI were constructed for prediction of revascularization; the optimal threshold values of each quantitative parameter were also determined (Fig. 7). All the ROC curves were above the reference line; the AUC, optimal threshold value, sensitivity, specificity, PPV, NPV, and accuracy of the quantitative parameters in predicting revascularization are shown in Table 8. The AUCs of the lesion-specific CT-FFR, distal-tip CT-FFR, and FAI were 0.798, 0.767, and 0.802, respectively. In cases where the optimal threshold value of the FAI was -86 HU, the sensitivity, specificity, PPV, NPV and overall accuracy in prediction of revascularization were 88.9%, 59.0%, 42.7%, 93.2%, and 0.66, respectively. The sensitivity, specificity, PPV, NPV, and overall accuracy of the lesion-specific CT-FFR for predicting revascularization were 73.6%, 81.0%, 56.3%, 88.2%, and 0.78, respectively (Table 8).

Discussion

To the best of our knowledge, this study was the first of its kind to compare the novel physiologic metric, CT-FFR, with the quantitative parameter, FAI, for prediction of coronary revascularization in real-world practice. In this study, the FAI, lesion-specific CT-FFR value, and distal-tip CT-FFR value were independent predictors of coronary revascularization. On comparing the CT-FFR and FAI in patients with CAD (as determined by CCTA), no differences in prediction accuracy were observed between the two parameters. In this context, the FAI showed a significant difference in diagnostic sensitivity, whereas the lesion-specific CT-FFR value showed the highest specificity.

Acute coronary syndrome (ACS) can be often the first manifestation of CAD, and is the major cause of death worldwide [3]. Vascular inflammation is recognized as a key factor to both plaque formation and rupture, which results in the occurrence of subsequent ACS [17]. Deposition of low-density lipoprotein and its oxidation in the coronary arterial wall triggers an inflammatory response, with recruitment of monocytes and T cells in the intima [1; 29]. Recent studies [2] have suggested that coronary inflammation drives dynamic changes in perivascular adipose tissue composition; this is identified by a novel CCTA-derived imaging biomarker, the perivascular FAI. In this context, inflammation-induced perivascular adipose tissue changes in adipocyte size and lipid content are related to CT attenuation gradients.

In our study, the sensitivity, specificity, PPV, NPV and overall accuracy in prediction of revascularization were 88.9%, 59.0%, 42.7%, 93.2%, and 0.66, respectively, when the optimal threshold value of FAI was -86 HU. The findings suggest that patients with lower uniformity and higher heterogeneity of PCAT have a high possibility of future ACS; this finding is consistent with that of the study by Shang et al [23]. Compared with other quantitative parameters, the FAI had the best sensitivity and NPV in our study; this may be attributed to its ability to reflect early pathophysiological changes of adipose tissue around the plaque.

The CT-FFR is widely used, as it is a new, noninvasive, and efficient assessment method for restrictive coronary artery stenosis [28]. This method is widely applied in clinical practice as it can provide both anatomical and physiological information regarding the coronary artery [31]. Many studies have reported that CT-FFR offers higher diagnostic accuracy than other non-invasive investigations for heart disease under the reference of the gold standard invasive FFR [4; 31]. In our study, the CT-FFR and FAI, as determined by CCTA in patients with CAD, did not show any difference in accuracy in predicting coronary revascularization. The modest per-vessel CT-FFR specificity detected in this study may be partly explained by the use of lesion-specific CT-FFR values rather than distal-tip CT-FFR values; however, this is not consistent with the results of the study by Rabbat et al. [22]. In this study, the lesion-specific CT-FFR showed better specificity and accuracy than the distal-tip CT-FFR in predicting revascularization; however, it had slightly lower sensitivity than the distal-tip CT-FFR. This predictor was also identified by Kruk et al. [14]. We also found the distal-tip CT-FFR value of all vessels to be slightly lower than that of the lesion-specific CT-FFR, regardless of the performance of revascularization; the latter was therefore more likely to provide false positive results.

Limitations

There are certain limitations to our study. The principal limitation lies in its retrospective nature, which may have resulted in selection bias among patients receiving ICA after CCTA; the results may have been different in patients receiving CCTA alone. Second, this was a single-center study; the results require further verification in large-sample multi-center studies. The cutoff values for the continuous variables identified by ROC curve analysis in the present study also require validation in future investigations. Additionally, only a proportion of patients (11%) received invasive FFR; in this context, our FFR utilization rate was consistent with real-world FFR utilization rates for intermediate lesions [20]. The use of FFR in all patients may help support the efficacy of the algorithm; however, as shown in our study, this may not reflect the real-world practice of revascularization [6]. In addition, stratified analysis could not be performed in this study owing to the lack of standard calcification scoring. Finally, the PCAT measurement used represented the mean CT attenuation of adipose tissue within the defined volume of interest, and was not weighted for technical or biological factors.

Conclusion

This study demonstrated the application value of the CT-FFR and FAI in predicting coronary revascularization in patients with documented CAD. There was similar overall accuracy between the CT-FFR and FAI. However, the FAI demonstrated a significant difference in diagnostic sensitivity, whereas the lesion-specific CT-FFR value showed the highest specificity. In conclusion, CT-FFR and FAI values obtained from quantitative CCTA improved the prediction of future revascularization. These parameters can potentially identify patients likely to receive revascularization on referral for cardiac catheterization.

Abbreviations

ICA= invasive coronary angiography

CCTA= coronary CT angiography

CAD= coronary artery disease

CT-FFR = fractional flow reserve derived from coronary computed tomography angiography ACS= acute coronary syndrome

PCAT= pericoronary adipose tissue

FAI= fat attenuation index

Declarations

Acknowledgements

We would like to acknowledge the reviewers for their helpful comments on this paper.

Author Contributions

Conceived and designed the experiments: FY TZ; Performed the experiments: CZ KS; Analyzed the data: FY; Contributed reagents/materials/analysis tools: YZ ; Wrote and submitted the paper: FY TZ. All authors read and approved the final version of the manuscript.

Consent for publication

Not applicable.

Ethics approval and consent to participate

The study was conducted in accordance with the Declaration of Helsinki (as revised in 2013), and was approved by the Medical Ethics Committee. The need for informed consent was waived for this retrospective study.

Conflict of interest

The authors declare no conflicts of interest.

References

1. Alexios S Antonopoulos MM, Patricia Coutinho, Cheerag Shirodaria, Costas Psarros, Laura Herdman, Fabio Sanna, Ravi De Silva, Mario Petrou, Rana Sayeed, George Krasopoulos, Regent Lee, Janet Digby, Svetlana Reilly, Constantinos Bakogiannis, Dimitris Tousoulis, Benedikt Kessler, Barbara Casadei, Keith M Channon, Charalambos Antoniades (2015 Jun) Adiponectin as a link between type 2 diabetes and vascular NADPH oxidase activity in the human arterial wall: the regulatory role of perivascular adipose tissue. *Diabetes*, 64(6):2207-2219
2. Antonopoulos AS, Sanna F, Sabharwal N, et al. (2017) Detecting human coronary inflammation by imaging perivascular fat. *Sci Transl Med*, 9(398)
3. Benjamin EJ, Virani SS, Callaway CW, et al. (2018) Heart Disease and Stroke Statistics-2018 Update: A Report From the American Heart Association. *Circulation*, 137(12):e67-e492
4. Coenen A, Kim YH, Kruk M, et al. (2018) Diagnostic Accuracy of a Machine-Learning Approach to Coronary Computed Tomographic Angiography-Based Fractional Flow Reserve: Result From the MACHINE Consortium. *Circ Cardiovasc Imaging*, 11(6):e007217
5. Cury RC, Abbara S, Achenbach S, et al. (2016) Coronary Artery Disease - Reporting and Data System (CAD-RADS): An Expert Consensus Document of SCCT, ACR and NASCI: Endorsed by the ACC. *JACC Cardiovasc Imaging*, 9(9):1099-1113
6. Dey D, Gaur S, Ovrehus KA, et al. (2018) Integrated prediction of lesion-specific ischaemia from quantitative coronary CT angiography using machine learning: a multicentre study. *Eur Radiol*, 28(6):2655-2664

7. Douglas PS, Hoffmann U, Patel MR, et al. (2015) Outcomes of anatomical versus functional testing for coronary artery disease. *N Engl J Med*, 372(14):1291-1300
8. Driessen RS, Danad I, Stuijzand WJ, et al. (2019) Comparison of Coronary Computed Tomography Angiography, Fractional Flow Reserve, and Perfusion Imaging for Ischemia Diagnosis. *J Am Coll Cardiol*, 73(2):161-173
9. Fossan FE, Muller LO, Sturdy J, et al. (2021) Machine learning augmented reduced-order models for FFR-prediction. *Comput Method Appl M*, 384
10. Goeller M, Tamarappoo BK, Kwan AC, et al. (2019) Relationship between changes in pericoronary adipose tissue attenuation and coronary plaque burden quantified from coronary computed tomography angiography. *Eur Heart J Cardiovasc Imaging*, 20(6):636-643
11. Han D, Liu JY, Sun ZH, Cui Y, He Y, Yang ZH (2020) Deep learning analysis in coronary computed tomographic angiography imaging for the assessment of patients with coronary artery stenosis. *Comput Meth Prog Bio*, 196
12. Hoshino M, Yang S, Sugiyama T, et al. (2020) Peri-coronary inflammation is associated with findings on coronary computed tomography angiography and fractional flow reserve. *J Cardiovasc Comput Tomogr*, 14(6):483-489
13. Investigators S-H, Newby DE, Adamson PD, et al. (2018) Coronary CT Angiography and 5-Year Risk of Myocardial Infarction. *N Engl J Med*, 379(10):924-933
14. Kruk M, Demkow M, Solecki M, Wardziak L, Kepka C (2018) The Location of Distal Coronary Artery Pressure Measurement Matters for Computed Tomography-Derived Fractional Flow Reserve. *JACC Cardiovasc Imaging*, 11(2 Pt 1):284-285
15. Kwan AC, McElhinney PA, Tamarappoo BK, et al. (2021) Prediction of revascularization by coronary CT angiography using a machine learning ischemia risk score. *Eur Radiol*, 31(3):1227-1235
16. Leipsic J, Abbara S, Achenbach S, et al. (2014) SCCT guidelines for the interpretation and reporting of coronary CT angiography: a report of the Society of Cardiovascular Computed Tomography Guidelines Committee. *J Cardiovasc Comput Tomogr*, 8(5):342-358
17. Momiyama Y, Adachi H, Fairweather D, Ishizaka N, Saita E (2014) Inflammation, Atherosclerosis and Coronary Artery Disease. *Clin Med Insights Cardiol*, 8(Suppl 3):67-70
18. Muller LO, Fossan FE, Braten AT, Jorgensen A, Wiseth R, Hellevik LR (2021) Impact of baseline coronary flow and its distribution on fractional flow reserve prediction. *Int J Numer Method Biomed Eng*, 37(11):e3246
19. Oikonomou EK, Marwan M, Desai MY, et al. (2018) Non-invasive detection of coronary inflammation using computed tomography and prediction of residual cardiovascular risk (the CRISP CT study): a post-hoc analysis of prospective outcome data. *The Lancet*, 392(10151):929-939
20. Parikh RV, Liu G, Plomondon ME, et al. (2020) Utilization and Outcomes of Measuring Fractional Flow Reserve in Patients With Stable Ischemic Heart Disease. *J Am Coll Cardiol*, 75(4):409-419
21. Patel MR, Peterson ED, Dai D, et al. (2010) Low diagnostic yield of elective coronary angiography. *N Engl J Med*, 362(10):886-895

22. Rabbat MG, Berman DS, Kern M, et al. (2017) Interpreting results of coronary computed tomography angiography-derived fractional flow reserve in clinical practice. *J Cardiovasc Comput Tomogr*, 11(5):383-388
23. Shang J, Ma S, Guo Y, et al. (2022) Prediction of acute coronary syndrome within 3 years using radiomics signature of pericoronary adipose tissue based on coronary computed tomography angiography. *Eur Radiol*, 32(2):1256-1266
24. Shaw LJ, Hausleiter J, Achenbach S, et al. (2012) Coronary computed tomographic angiography as a gatekeeper to invasive diagnostic and surgical procedures: results from the multicenter CONFIRM (Coronary CT Angiography Evaluation for Clinical Outcomes: an International Multicenter) registry. *J Am Coll Cardiol*, 60(20):2103-2114
25. Tanaka K, Bezerra HG, Gaur S, et al. (2016) Comparison Between Non-invasive (Coronary Computed Tomography Angiography Derived) and Invasive-Fractional Flow Reserve in Patients with Serial Stenoses Within One Coronary Artery: A NXT Trial substudy. *Ann Biomed Eng*, 44(2):580-589
26. Taylor CA, Fonte TA, Min JK (2013) Computational fluid dynamics applied to cardiac computed tomography for noninvasive quantification of fractional flow reserve: scientific basis. *J Am Coll Cardiol*, 61(22):2233-2241
27. Tesche C, De Cecco CN, Albrecht MH, et al. (2017) Coronary CT Angiography-derived Fractional Flow Reserve. *Radiology*, 285(1):17-33
28. Tesche C, De Cecco CN, Baumann S, et al. (2018) Coronary CT Angiography-derived Fractional Flow Reserve: Machine Learning Algorithm versus Computational Fluid Dynamics Modeling. *Radiology*, 288(1):64-72
29. Wolf D, Ley K (2019) Immunity and Inflammation in Atherosclerosis. *Circ Res*, 124(2):315-327
30. Yu M, Dai X, Deng J, Lu Z, Shen C, Zhang J (2020) Diagnostic performance of perivascular fat attenuation index to predict hemodynamic significance of coronary stenosis: a preliminary coronary computed tomography angiography study. *Eur Radiol*, 30(2):673-681
31. Zhang JM, Han H, Tan RS, et al. (2021) Diagnostic Performance of Fractional Flow Reserve From CT Coronary Angiography With Analytical Method. *Front Cardiovasc Med*, 8:739633

Tables

Tables 1 to 8 are available in the Supplementary Files section.

Figures

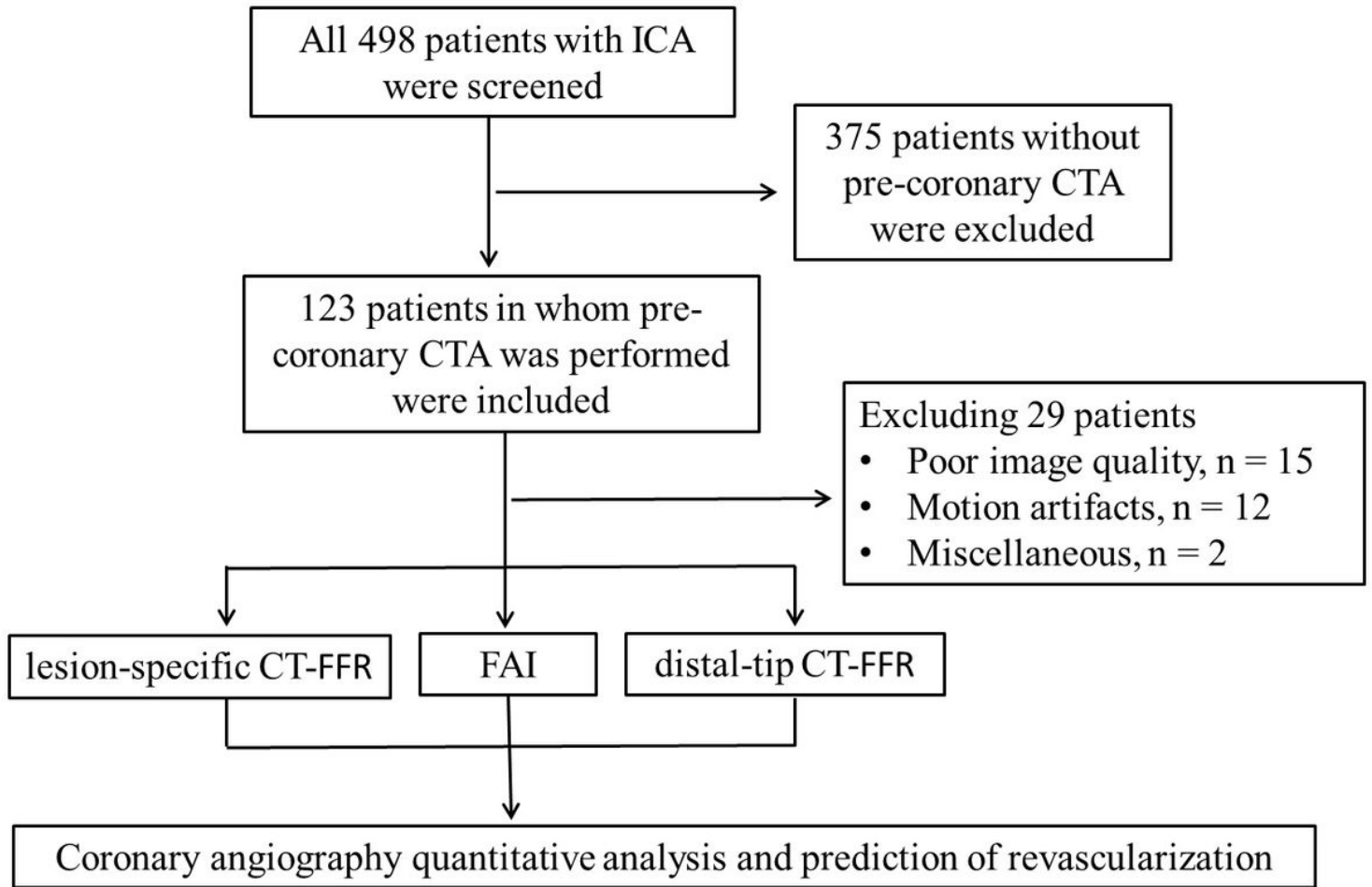


Figure 1

Study population flow chart. ICA, invasive coronary angiography; CTA, computed tomography angiography; CT-FFR, fractional flow reserve derived from coronary computed tomography angiography; FAI, fat attenuation index.

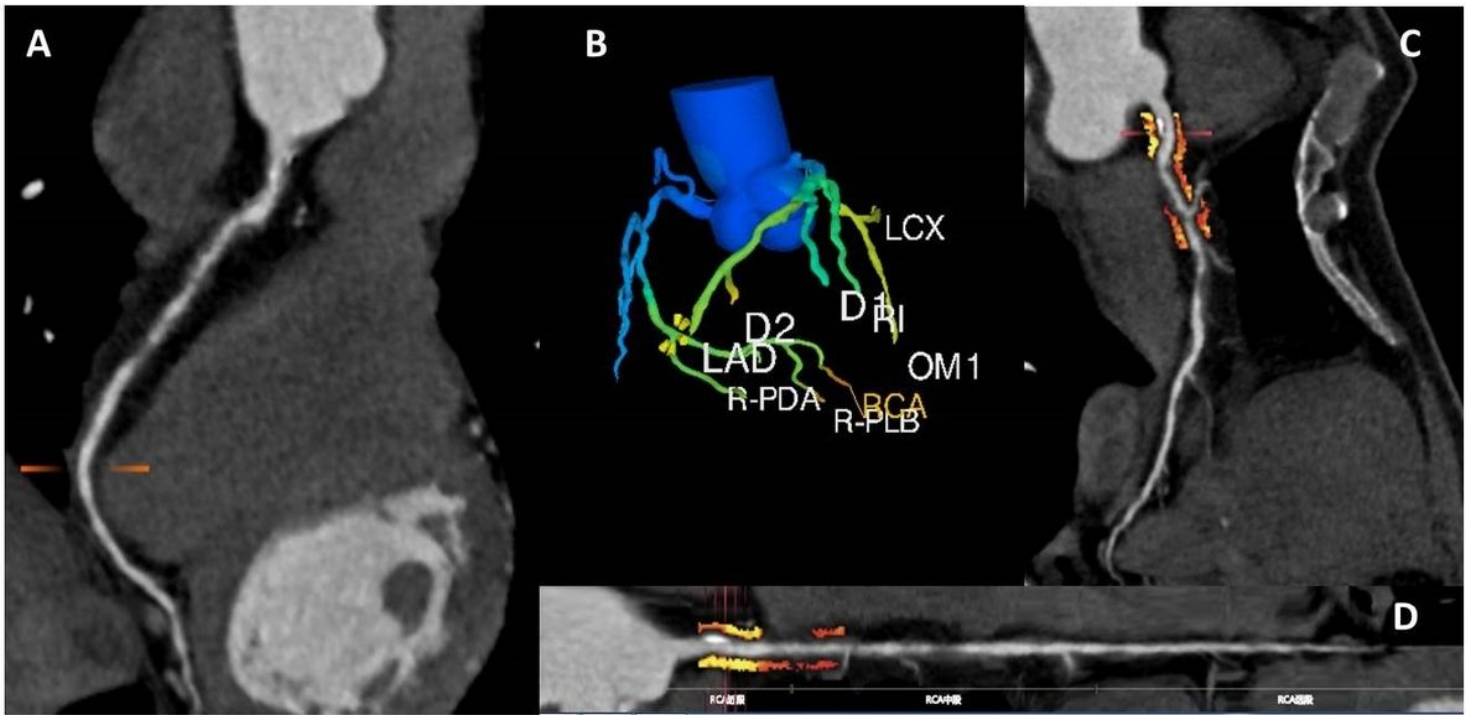


Figure 2

The procedure for performing CT-FFR and FAI measurements. The right coronary artery with 90% stenosis was revascularized by ICA. (A) CCTA demonstrates the right coronary artery with severe stenosis. (B) The CT-FFR value was obtained from the corresponding CT-FFR model derived from the CCTA image. The lesion-specific CT-FFR and distal-tip CT-FFR values are 0.76 and 0.66, respectively. (C) and (D) PCAT quantification within a diameter of 3 mm around the proximal RCA (straightened view); the PCAT is visualized using the adipose tissue Hounsfield unit color table, shown with the color bar. The FAI was defined as the mean CT attenuation of PCAT in the traced 40-mm segment on crude analysis. The FAI is seen to be -76HU. ICA, invasive coronary angiography; CCTA, coronary computed tomography angiography; CT-FFR, fractional flow reserve derived from coronary computed tomography angiography; PCAT, pericoronary adipose tissue; FAI, fat attenuation index.

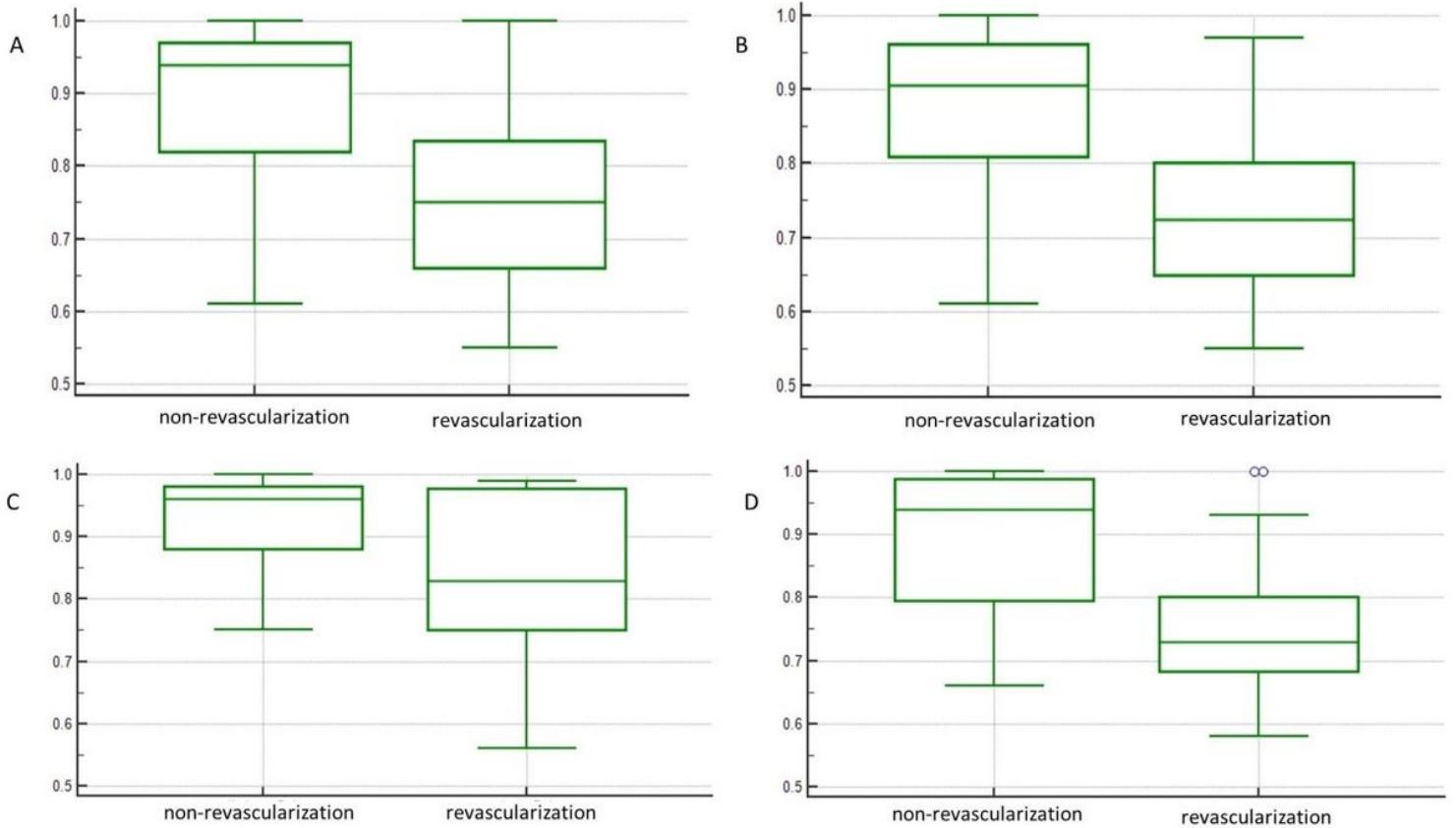


Figure 3

Box-and-whisker plots for comparison of differences in lesion-specific CT-FFR between revascularization and non-revascularization groups (A) for all vessels, (B) for LAD, (C) for LCx, (D) for RCA. The mean lesion-specific CT-FFR value in the revascularization group was lower than that in the non-revascularization group, across all vessels and the sub vascular groups. CT-FFR, fractional flow reserve derived from coronary computed tomography angiography; LAD, left anterior descending; LCx, left circumflex; RCA, right coronary artery.

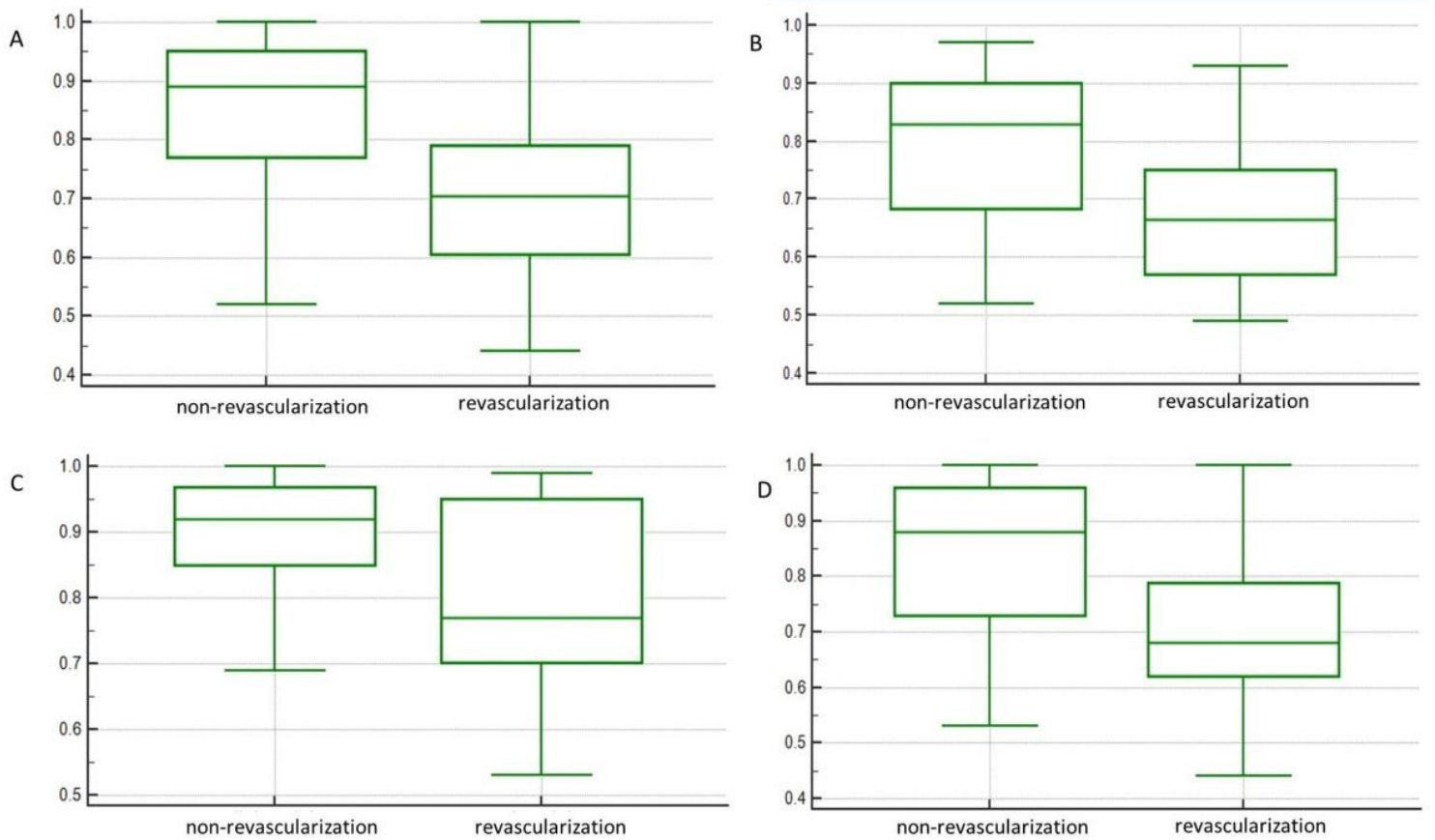


Figure 4

Box-and-whisker plots for comparison of distal-tip CT-FFR difference between revascularization and non-revascularization groups (A) for all vessels, (B) for LAD, (C) for LCx, (D) for RCA. The mean distal-tip CT-FFR value in the revascularization group was lower than that in the non-revascularization group, across all vessels and the sub vascular groups. CT-FFR, fractional flow reserve derived from coronary computed tomography angiography; LAD, left anterior descending; LCx, left circumflex; RCA, right coronary artery.

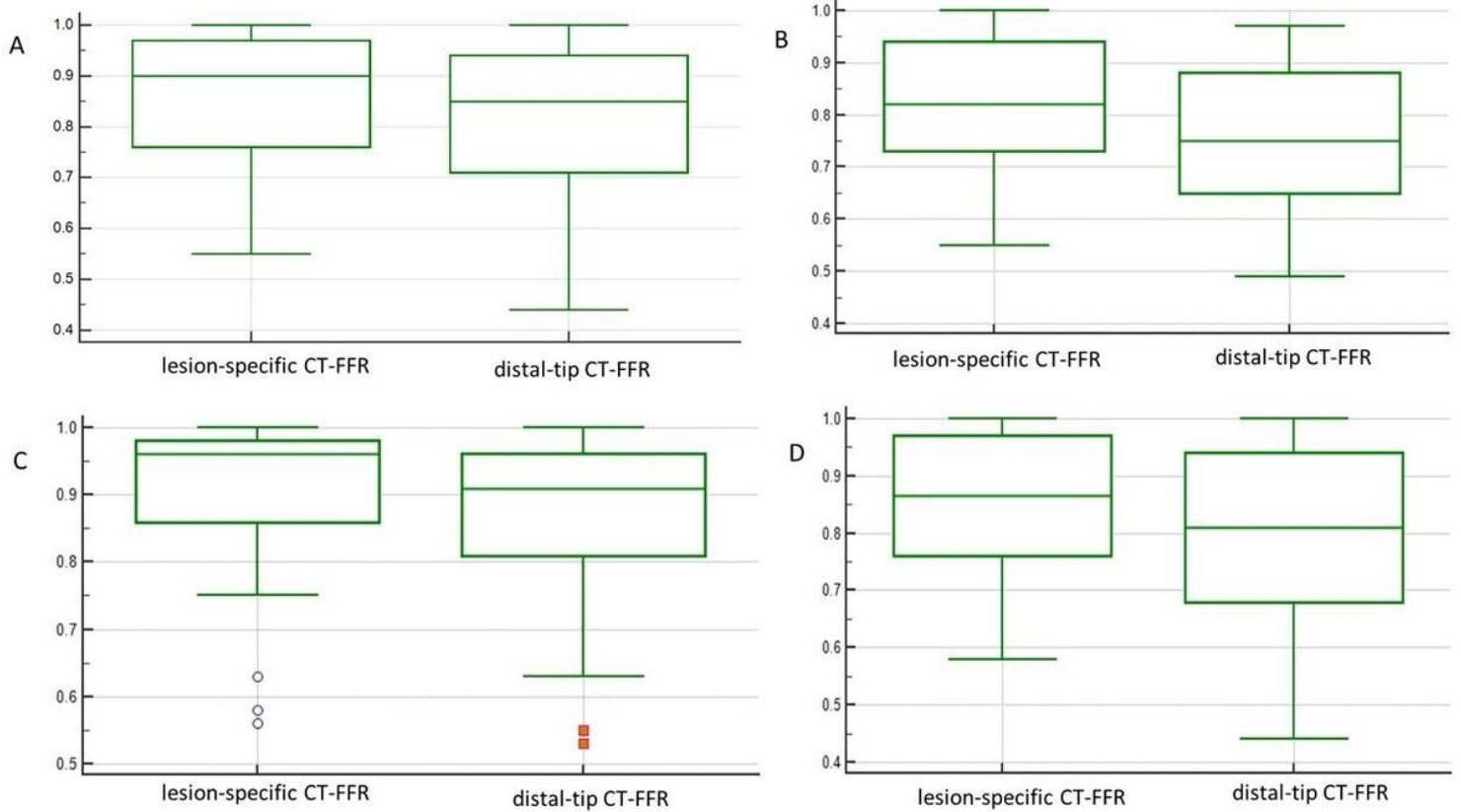


Figure 5

Box-and-whisker plots for comparison of differences in lesion-specific CT-FFR and distal-tip CT-FFR (A) for all vessels, (B) for LAD, (C) for LCx, (D) for RCA. The mean lesion-specific CT-FFR was higher than the lesion-specific CT-FFR in all vessels and sub vascular groups. CT-FFR, fractional flow reserve derived from coronary computed tomography angiography; LAD, left anterior descending; LCx, left circumflex; RCA, right coronary artery.

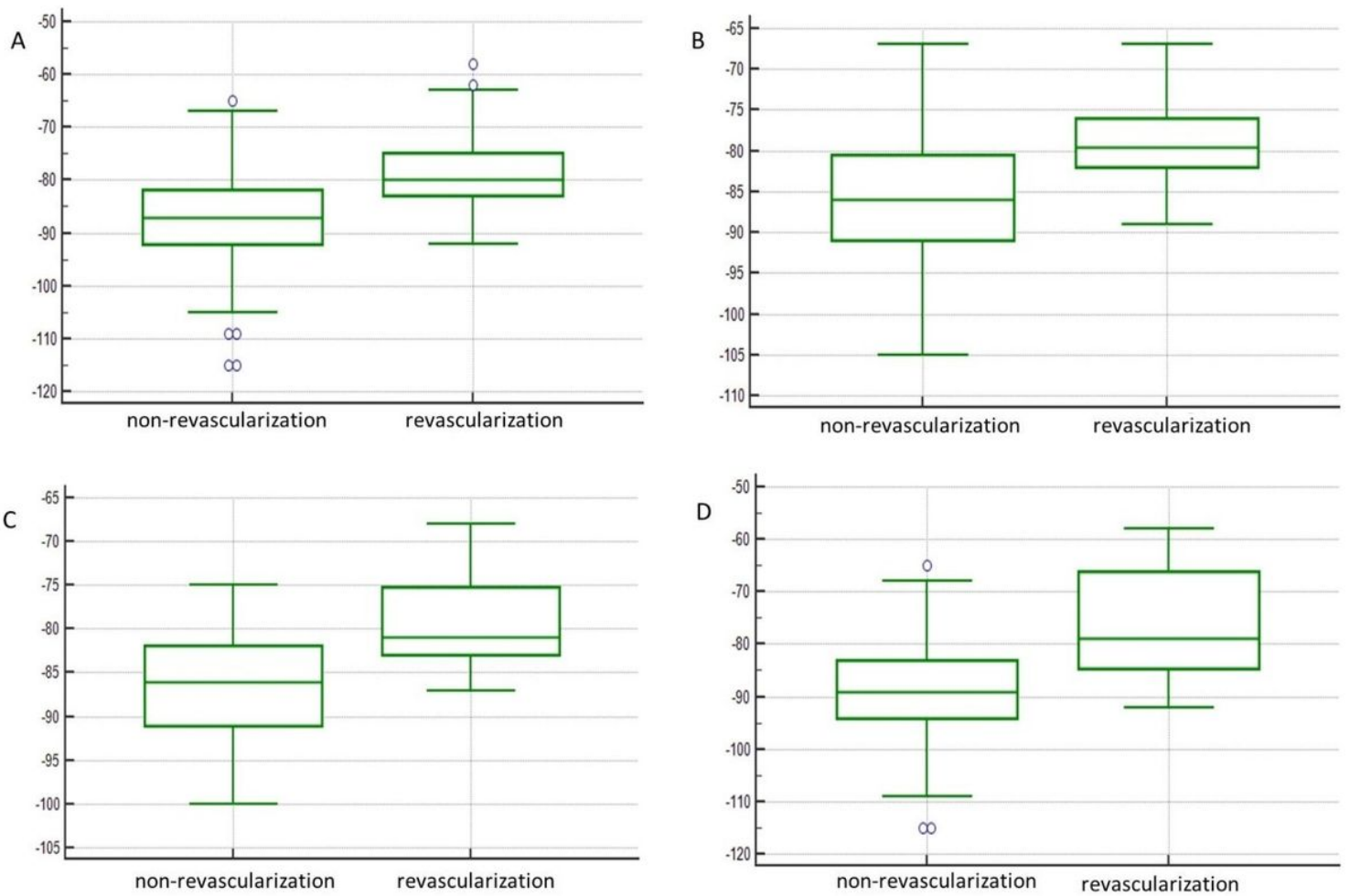


Figure 6

Box-and-whisker plots for comparison of differences in FAI between revascularization and non-revascularization groups (A) for all vessels, (B) for LAD, (C) for LCx, (D) for RCA. The mean FAI value in the revascularization group was higher than that in the non-revascularization group, across all vessels and the sub vascular groups. FAI, fat attenuation index; LAD, left anterior descending; LCx, left circumflex; RCA, right coronary artery.

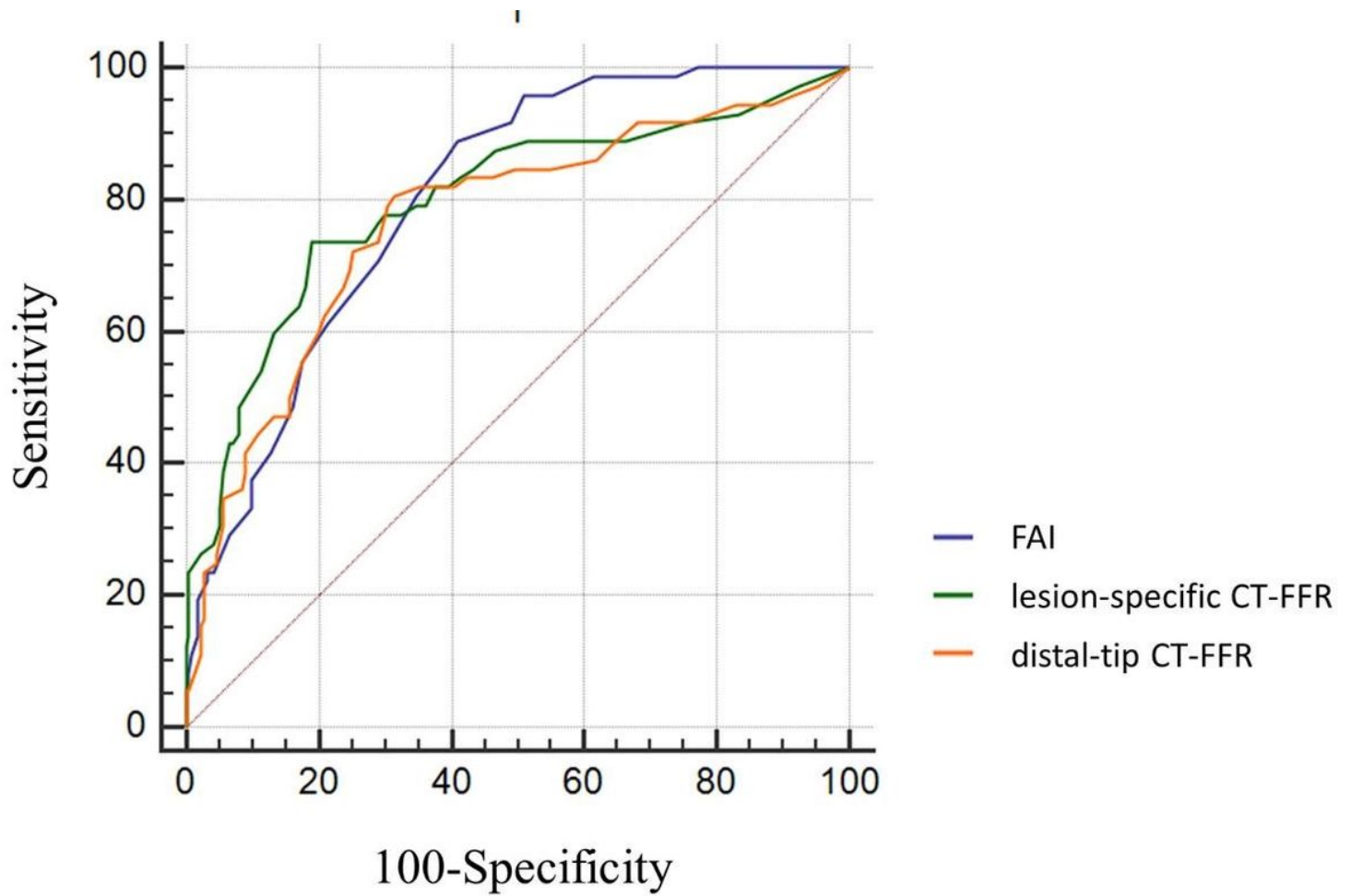


Figure 7

Graphs showing receiver operating characteristic curves of quantitative parameters derived from CCTA for prediction of standard-of-care-guided coronary revascularization. The area under the ROC curve of the FAI is the largest (= 0.802). All ROC curves are above the reference line. FAI fat attenuation index; CT-FFR, fractional flow reserve derived from coronary computed tomography angiography.

Supplementary Files

This is a list of supplementary files associated with this preprint. Click to download.

- [table.docx](#)